ChemComm

Accepted Manuscript

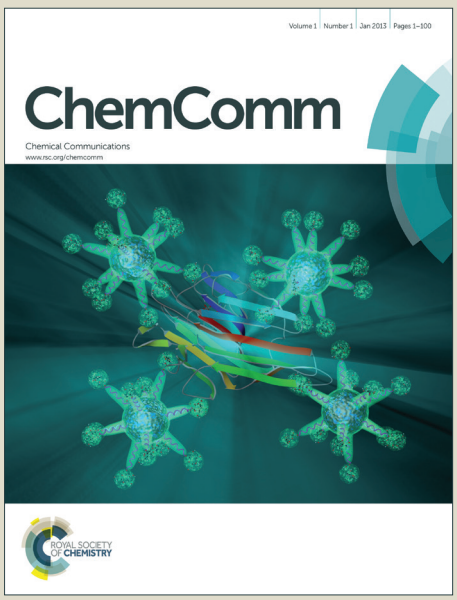

ROYAL SOCIETY OF CHEMISTRY

www.rsc.org/chemcomm

ChemComm

COMMUNICATION

Helix Handedness Inversion in Arylamide Foldamers: Elucidation and Free Energy Profile of a Hopping Mechanism

Received 00th January 20xx,
Accepted 00th January 20xx

DOI: 10.1039/x0xx00000x

www.rsc.org/

Ara M. Abramyan, Zhiwei Liu and Vojislava Pophristic*

We report the first atomistic level description of the handedness inversion mechanism for helical arylamide foldamers. The key process in the handedness inversion is simultaneous unfolding and folding of two adjacent aryl-aryl linkages, propagating from a helix terminus along the strand. Intermediates along the inversion pathway have a common feature - a single unfolded aryl-aryl linkage (through C_{aryl}-C_{amide} rotation) connecting two helical segments of opposite handedness. This explicit solvent metadynamics study also provides thorough quantitative free energy information for each step of the previously uncharacterized inversion pathway.

Chirality is a critical structural feature for a variety of chemical entities, with particularly prominent roles in folding and establishing the ultimate shape and function of natural and synthetic polymers. Consequently, chirality of the ubiquitous helix motif has been an intriguing research topic in synthetic chemistry for decades.[1] Recent developments in computer technology and methodologies provide a currently under-utilized opportunity to build on pioneering work of Green,[2] and reveal explicit, atomistic level information about mechanisms and energetics of helix handedness inversion, which is inaccessible experimentally. A major challenge lies in the adaptation of computational tools originally developed for biopolymers. Here, we present free energy molecular dynamics (MD) elucidation of handedness inversion mechanism for a representative of a large helical foldamer class. From both experimental and computational aspects, foldamers, non-natural oligomers that adopt stable secondary structure in solution,[1b,3] are particularly attractive for systematic studies of helix chirality.[4] This stems from their unlimited "helical codon" basis,[5] which allows for a high level of versatility and control over the resulting conformations.[4a,6] Handedness of helical foldamers, in particular arylamide-based ones, has therefore been a subject of a focused and fast-expanding experimental exploration in the past decade.[4b,7] This effort has however not been accompanied by a complementary computational activity, as it requires suitable force field optimizations, an effort our group has undertaken recently.[8]

Free energy MD methods are of particular interest for exploring handedness inversion mechanism, because they can yield detailed reaction pathways and associated energetics.[9] However, they have been only scarcely used to study these problems.[10] The main obstacle in applying these methods to complex systems is the practical limitation of up to only two to three collective variables (CVs), which have to be chosen to drive the free energy surface exploration in the direction of a targeted reaction path, i.e. the process outcome.[11] We designed our CVs to be inherently related to the helix secondary structure and backbone conformation. Thus our CVs have a direct and clearly defined relationship with the geometrical variables that drive the folding/unfolding process at the primary structure (i.e. sequence) level. The resulting reaction path and energetics thus reveal specific backbone torsions that are responsible for helix handedness inversion. Furthermore, for these arylamide systems, relatively short helices are representative of longer helices, allowing for information transferability and generality of our conclusions.[8c] Finally, our endeavour involved recently optimized parameters, necessary for accurate MD simulations of arylamide foldamers.[8c,8g]

Using this approach, we have deciphered and now report the hopping mechanism of arylamide helix inversion.[7i] This study reveals, for the first time, atomistic level insight into the structure of the inversion center, backbone internal bond rotations that drive the propagation mechanism, and their cooperation. In particular, we show how helix handedness reversal propagates through the simultaneous unfolding of one monomer-monomer linkage and refolding of the adjacent one.

In this work, we focus on helical arylamides derived from 8-amino-2-quinolinecarboxilic acid because of their remarkable stability and consequent availability of extensive experimental information,[7g,7i,j,12] including conformational characterization in solution and kinetic data on handedness inversion. Using various experimental techniques, Huc and coworkers have determined the kinetic rate constants and free energy barriers for racemization of these oligomers ranging from a hexamer to a hexadecamer at different temperatures.[7i] The results led to a hypothesis that the oligomers do not fully unfold during handedness inversion; instead, a hopping mechanism was suggested in which a local inversion center, separating two helical segments of opposite handedness, propagates along the strand from one end to another. The general features of the mechanism have been supported for related systems.[2,5,13]

Department of Chemistry & Biochemistry, University of the Sciences
600 South 43rd Street, Philadelphia, PA 19104, USA
Fax: 215-596-8543
E-mail: v.pophri@usciences.edu.
Electronic Supplementary Information (ESI) available: details of simulation setup, quantum mechanical potential energy profiles of arylamide model compounds, additional FEPs (end-to-end distance as one of the CVs, different solvents), error analysis. See DOI: 10.1039/x0xx00000x

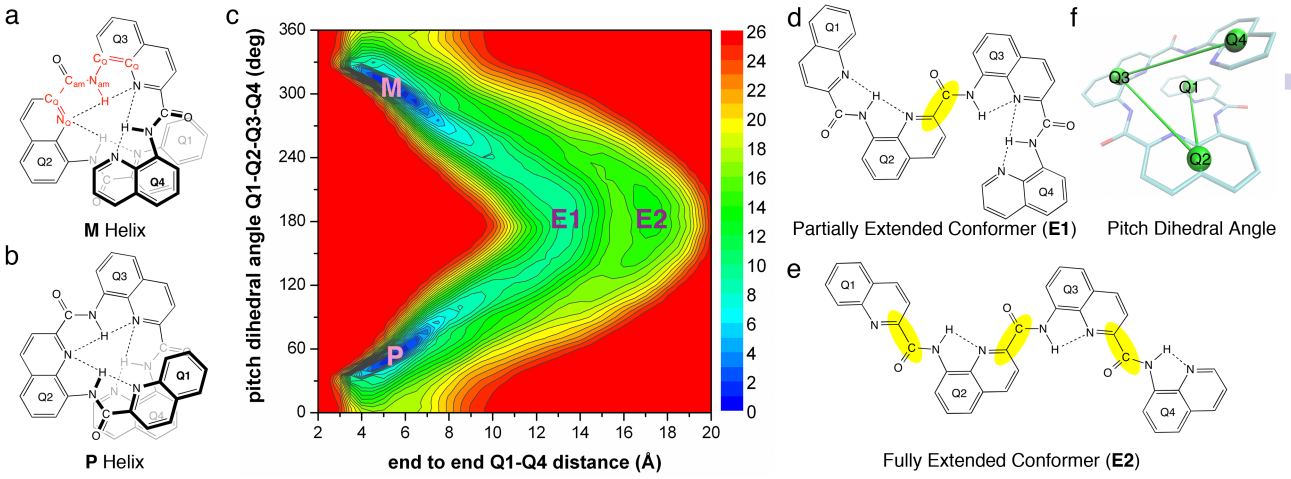

Fig. 1. (a, b) Structures of the left (**M**) and right (**P**) handed quinoline based tetramer helices. The definitions of the N_Q-C_Q-C_{am}-N_{am} and C_Q-C_Q-N_{am}-H dihedral angles are shown in red in the **M** helix structure. Dotted lines in structures indicate H-bonds; (c) Free energy profile (kcal/mol) with respect to the end-to-end Q1-Q4 distance and pitch dihedral angle Q1-Q2-Q3-Q4 of the tetramer in chloroform; (d, e) Structures of the partially and fully extended conformers. Highlighted in yellow are the bonds that rotated ~180° from the helical structure values; (f) Pitch dihedral angle, defined by centers of masses of four consecutive quinoline rings.

Utilizing force field parameters specifically optimized for the quinoline based arylamides (Fig. 1), we carried out all-atom MD simulations (300 to 500 ns) in explicit solvents (chloroform and water), combined with the metadynamics free energy method[9] on tetramer, pentamer and hexamer helices. The method accelerates simulation by adding small repulsive potentials ("hills") to the underlying free energy landscape, thus gradually biasing the system to escape energy minima and explore wide conformational space. Concurrently, it maps out the free energy surface as the negative of the accumulated sum of hills. From metadynamics simulations, we determined free energy of the three oligomers with respect to two CVs to generate two-dimensional free energy profiles (FEPs). CVs were chosen as follows. The pitch dihedral angle (Fig. 1f), defined by the centers of masses (COMs) of four consecutive quinoline rings ("Q"), identifies the handedness of the helix: positive dihedral angle for right-handed (**P**) and negative angle for left-handed (**M**) helices. Therefore, at least one pitch dihedral angle was used as a CV in each metadynamics run. We carried out two sets of simulations, differing in the choice of the second CV. In *set 1* simulations, the end-to-end distance (between COMs of the terminal aromatic rings) was used as the second CV, to examine the extent of helical unfolding during handedness inversion. In *set 2* simulations, the second CV is another pitch dihedral angle, giving insight to local conformational information of intermediates along the inversion pathway. Here we focus on our findings in chloroform, as the discussed mechanism remains the same in both solvents.

Fig. 1c shows the FEP for handedness inversion of a tetramer, which has close to 1.5 turns and one pitch dihedral angle (∠Q1-Q2-Q3-Q4, Fig. 1f). The handedness inversion does not require the tetramer to fully extend (i.e. to turn into **E2**, Fig. 1e); the more energetically accessible inversion path goes via an end-to-end distance of only ~13 Å and a barrier of ~9.5 kcal/mol (through the partially extended **E1** conformer, Fig. 1d).

At the atomistic level, **P** and **M** helices differ in the distribution of backbone dihedral angles N_Q-C_Q-C_{am}-N_{am} and C_Q-C_Q-N_{am}-H (Fig. 1a). The accumulation of the six slightly positive (or negative) atomistic level aryl-amide torsions (two per amide bond, see Fig. 2) results in an overall positive (or negative) pitch dihedral angle (60° or -60°, which is equivalent to 300°) in the folded helical structur In both **P** and **M** helices, the atomistic dihedral angles are close to 0°, indicating intramolecular hydrogen-bond (H-bond) between th endocyclic N_Q and the amide proton. The inversion of the handedness requires a slight positive to negative (or vice ver shift of the atomistic dihedral angle. In principle, this can occ either through 0°, which is energetically effortless, or through 180 which requires breaking of the intramolecular H-bond and conjugation (Fig. S1).

In helical oligomers, however, steric clashes between stacked aromatic units (e.g. Fig. 1a,b,f Q1 and Q4) make rotation of C_Q-C or C_Q-N_{am} through 0° improbable. Handedness inversion of tetramer, therefore, occurs via **E1** with ∠Q1-Q2-Q3-Q4 = 180° (Fi 1c,d). It should be noted that the inversion of Q2-amide-Q requires only one of the two aryl-amide bonds (C_{Q2}-C_{am} or C_{Q3}-N to rotate to 180°. Detailed conformational analysis of **E1** indic that 180° rotation occurs exclusively around the C_{Q2}-C_{am} bond (highlighted in yellow, Fig. 1d) whereas the N_{am}-C_{Q3} linkage maintains the H-bonded conformation. This is consistent with o quantum mechanical results (Fig. S1) in which a 180° rotatio around the C_Q-N_{am} bond has a higher barrier than an analogou rotation around the C_Q-C_{am} bond.

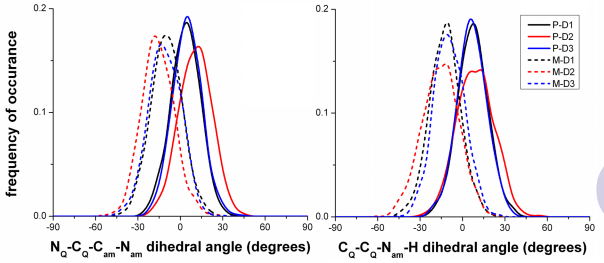

Fig. 2. The distribution of the atomistic N_Q-C_Q-C_{am}-N_{am} and C_Q-C_Q-N_{am}-H dihedral angl in the **M** and **P** helical conformers collected from 300 ns simulation of tetramer chloroform. D1, D2 and D3 denote atomistic dihedral angles between Q1 and Q2, Q2 and Q3, and Q3 and Q4 (Fig. 1), respectively.

The 180° rotation of the C_{Q2}-C_{am} bond opens up the stacke aromatic units Q1 and Q4 (Fig. 1d). Therefore, from intermedia **E1**, no additional 180° rotations are necessary for the remaining

five aryl-amide torsions (two pairs at the termini and N_{am}-C_{Q3}) for the tetramer to invert its handedness. The torsions now can easily adjust from slightly positive to slightly negative values (or vice versa) through 0° while maintaining the intramolecular H-bonds. As evidenced by Fig. 1c, the fully extended conformer (**E2**), in which both C_{Q1}-C_{am} and C_{Q3}-C_{am} rotate by 180°, is higher in energy and not a necessary state for the handedness inversion of tetramer.

For both pentamer and hexamer, the FEPs from *set 1* metadynamics simulations (Fig. S2) show that the largest end-to-end distance and the highest energy along the inversion pathways are ~14 Å and ~14-16 kcal/mol, respectively. The fact that the largest end-to-end distances of pentamer and hexamer are comparable to the **E1** of tetramer suggested that their handedness inversion also goes through partially extended intermediates. To decipher their inversion pathways, we ran *set 2* simulations, with two pitch dihedral angles used as CVs.

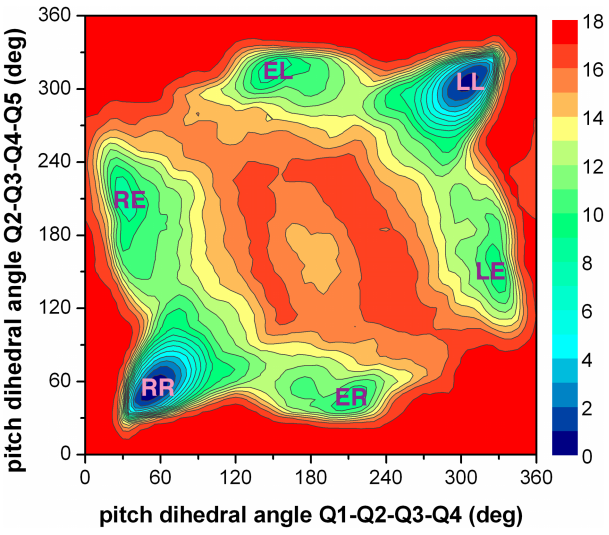

Fig. 3. Pentamer free energy profile (energy in kcal/mol) with respect to its pitch dihedral angles Q1-Q2-Q3-Q4 and Q2-Q3-Q4-Q5, in chloroform. Note that **LL** and **RR** correspond to **M** and **P**, respectively.

Fig. 3 shows the FEP of pentamer handedness inversion as a function of its two pitch dihedral angles. We labelled the minima and intermediates based on the states of the two central aryl-aryl linkages, i.e. the two corresponding pitch dihedral angles. The "**R**" (right) state corresponds to a pitch dihedral angle centered at ~60°, "**E**" (extended) to ~180° and "**L**" (left) to ~300°. There are two global minima, **RR** (**P**) and **LL** (**M**), and two inversion pathways involving the **RE** and **EL** local minima in one (Fig. 3, upper left), and **ER** and **LE** in the other case (Fig. 3, lower right). Each local minimum has one extended (**E**) and one folded (**L** or **R**) aryl-aryl linkage and lies ~8.3 kcal/mol (**RE**, **EL**) or ~9.3 kcal/mol (**ER**, **LE**) above the global minima. The **RR↔RE↔EL↔LL** pathway features transition states with energies of ~11.5, ~15.0 and ~12.0 kcal/mol. The **RR↔ER↔LE↔LL** pathway (Fig. 4) has transition states at ~12.0, ~16.0 and ~12.3 kcal/mol. A ~1 kcal/mol difference between the two pathways (above the FEP's estimated error of ~0.55 kcal/mol, Fig. S6), stems from the N to C asymmetry of the helix and is also observed in the hexamer FEP (see below). Inversion from N-terminus thus slightly differs from inversion from C-terminus. Clearly, both pathways (**RR↔RE↔EL↔LL** and **RR↔ER↔LE↔LL**) follow the general mechanism in which the helix undergoes local inversion that starts at one end and propagates to the other. The most important finding about the pentamer inversion pathway lies in the **RE↔EL** and **ER↔LE** transition steps, i.e. simultaneous folding of one aryl-aryl linkage while its neighbouring aryl-aryl linkage unfolds (Fig. 4). Finally, at the atomistic level, similarly to tetramer, the **R→E** and **L→E** transitions are almost exclusively achieved by the 180° rotation of the C_Q-C_{am} bonds.

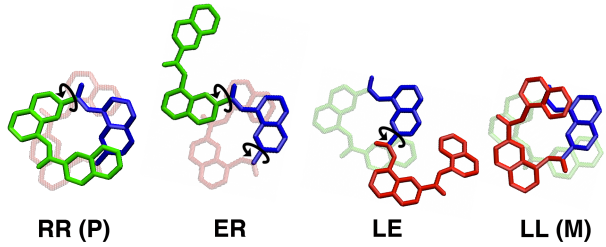

Fig. 4. Snapshots from metadynamics simulation of pentamer, showing the handedne inversion mechanism and characteristic conformers on the **RR↔ER↔LE↔LL** pa Monomers are coloured differently for clarity; Q1 and Q2 are green, Q3 is blue, Q4 and Q5 are red. Black arrows indicate 180° rotation of the C_Q-C_{am} bonds, leading t subsequent conformer along the pathway.

Fig. 5 shows the FEP for the hexamer handedness inversion as a function of its pitch dihedral angles Q1-Q2-Q3-Q4 (N-terminal) and Q3-Q4-Q5-Q6 (C-terminal). The energy difference between the tw global minima (**RRR** (**P**) and **LLL** (**M**)) is less than 0.1 kcal/mol, indicating sufficient conformational sampling. In order to reve information about the middle pitch dihedral angle Q2-Q3-Q4-Q5, we extracted the conformations from each minimum basin (1 kcal/mol around the minimum), from the 500 ns MD trajectory. These conformations were analyzed and labelled using **R**, **E**, **L** base on the folded *vs* unfolded states of the three aryl-aryl linkages associated with the three pitch dihedral angles.

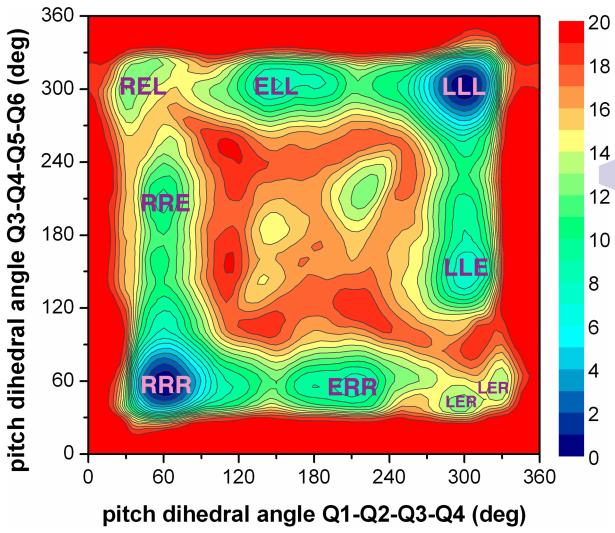

Fig. 5. Hexamer free energy profile (energy in kcal/mol) with respect to its pitch dihedral angles Q1-Q2-Q3-Q4 and Q3-Q4-Q5-Q6, in chloroform. Note that **LLL** and correspond to **M** and **P**, respectively.

There are seven local minima, each corresponding to a sta where only one aryl-aryl linkage is unfolded. In the case of th **LER/REL** minima, both **L** and **R** components are presen Furthermore, there are two **LER** minima (Fig. 5), one reached v C_{Q3}-C_{am} 180° rotation (lower in energy), the other via C_{Q4}-N_{am} 180° rotation. Similarly to pentamer, the unwinding starts at one end a global minimum conformer (**RRR** or **LLL**). As pitch dihedral angle

Q1-Q2-Q3-Q4 or Q3-Q4-Q5-Q6 unfolds and overcomes a ~11-12 kcal/mol barrier, the conformer converts to **ERR** (or **RRE**) if started from **RRR**, or **ELL** (or **LLE**) if started from **LLL**. These states have an elevated energy of ~7-10 kcal/mol. The local inversion center (the **E** state) then propagates to the next pitch dihedral angle (the central Q3-Q4 linkage), whereas the previously unfolded pitch dihedral angle folds to the inverted state. These propagations, i.e. the **ER**R↔**LE**R, R**RE**↔R**EL**, **EL**L↔**RE**L and L**LE**↔L**ER** transitions, are essentially the same as those observed in pentamer (**RE**↔**EL** and **ER**↔**LE**). This process of simultaneous folding and unfolding of adjacent aryl-aryl linkages has barrier of ~16-17 kcal/mol. The resulting **LER** and **REL** states are at ~12-13 kcal/mol and have opposite handedness on the two sides of the unfolded linkage. This leads to the two inversion pathways: **RRR**↔**RRE**↔**REL**↔**ELL**↔**LLL** and **RRR**↔**ERR**↔**LER**↔**LLE**↔**LLL**. Finally, as in the pentamer case, the asymmetry of the helix results in the first pathway being slightly more energetically favorable.

The highest energy barrier of ~16-17 kcal/mol for hexamer handedness inversion (at 300 K) agrees with the experimentally measured Gibbs activation energy of 20.6 kcal/mol at 283 K.[7i] The difference comes from the fact that, in the experiments, 4-quinoline isobutoxyl groups are attached to the outer rim of the helix, adding extra steric hindrance to the helix inversion and thus increasing its barrier. In addition, the different temperature and solvents used (chloroform vs chloroform/hexane) might also contribute to the discrepancy. Indeed, solvent-dependency study[12] has shown that both highly non-polar and protic polar solvents enhance stability of the quinolone-based helices. Our metadynamics simulations in water (ESI) show an increase in inversion barriers with respect to chloroform, due to the solvophobic stabilization of the folded structure. Importantly, in our simulations, the increase of the highest barrier on the inversion pathway from pentamer to hexamer is ~1 kcal/mol, in parallel to the experimentally observed < 1 kcal/mol increase associated with the growth of oligomer by one unit in the hexamer to hexadecamer series.[7i] Furthermore, the equilibrated helical structures in our simulations agree well with experimental ones in terms of helical pitch (~3.5 Å) and number of units per turn (2.5).[7i,14] Finally, our results directly confirm previously postulated hopping mechanism[2,5,7i,13a] and translate these "coarse grained" models to explicit backbone bond rotations.

In conclusion, we identified atomistic level motions that govern a stepwise unfolding-folding pathway for helical arylamides (Fig. 4), and determined associated free energy profiles. The initial step of the hopping mechanism is the unwinding of the 2nd (or 2nd to the last) aryl-aryl linkage, almost exclusively via the C_Q-C_{am} 180° rotation, to form an intermediate with a single unfolded aryl-aryl linkage. The inversion is then followed by successive propagation steps; in each step, the unfolded linkage folds into the opposite handedness accompanied by simultaneous unwinding of the next aryl-aryl linkage. The process can be generalized as follows: $\mathbf{R_n \leftrightarrow R_{n-1}E \leftrightarrow R_{n-2}EL \ldots R_{n-m}EL_{m-1} \ldots REL_{n-2} \leftrightarrow EL_{n-1} \leftrightarrow L_n}$, where n is the total number of pitch dihedral angles (number of monomers in the oligomer minus 3) and m is the step in the conversion from **R** to **L** helix. This mechanism involves the breakage of the fewest H-bonds and the minimal disturbance of aromatic stacking. A longer oligomer has to go through more steps to completely inverse its handedness; however, the energy barrier at each step is not significantly affected by the length of the oligomer, in agreement with experimental measurements.[7i] Studies on the energetics and mechanism of handedness control by addition of a chiral biasing group on folding/unfolding of helical arylamide foldamers are underway.

This research was supported by the NSF MSN-1049771 and MRI CHE-1229564 grants.

Notes and references

1. (a) J. Cornelissen, A. E. Rowan, R. J. M. Nolte and N. Sommerdijk, *Chem. Rev.*, 2001, **101**, 4039; (b) D. J. Hill, M. J. Mio, R. B. Prince, T. S. Hughes and J. S. Moore, *Chem. Rev.*, 2001, **101**, 3893; (c) T. Nakano and Y. Okamoto, *Chem. Rev.*, 2001, **101**, 4013; (d) E. Yashima, K. Maeda, H. Iida, Y. Furusho and K. Nagai, *Chem. Rev.*, 2009, **109**, 6102.
2. (a) M. M. Green, J. W. Park, T. Sato, A. Teramoto, S. Lifson, R. L. B. Selinger and J. V. Selinger, *Angew. Chem. Int. Ed.*, 1999, **38**, 3139; (b) S. Lifson, C. E. Felder and M. M. Green, *Macromolecules*, 1992, **25**, 4142.
3. (a) S. H. Gellman, *Acc. Chem. Res.*, 1998, **31**, 173; (b) K. C. M. Goodman, S. Choi, S. Shandler and W. F. DeGrado, *Nat. Chem. Biol.*, 2007, **3**, 252.
4. (a) S. Hecht and I. Huc, eds., *Foldamers: Structure, Properties, and Applications*, Wiley-VCH, Weinheim, 2007; (b) D.-W. Zhang, X. Zhao, J.-L. Hou and Z.-T. Li, *Chem. Rev.*, 2012, **112**, 5271.
5. M. Ohkita, J. M. Lehn, G. Baum and D. Fenske, *Chem. Eur. J.*, 1999, **5**, 3471.
6. (a) G. Guichard and I. Huc, *Chem. Commun.*, 2011, **47**, 5933; (b) B. Gong, *Acc. Chem. Res.*, 2008, **41**, 1376.
7. (a) I. Saraogi and A. D. Hamilton, *Chem. Soc. Rev.*, 2009, **38**, 1726; (b) R. A. Brown, V. Diemer, S. J. Webb and J. Clayden, *Nat. Chem.*, 2013, **5**, 853; (c) J. Maury, B. A. F. Le Bailly, J. Raftery and J. Clayden, *Chem. Commun.*, 2015, **51**, 11802; (d) L. Byrne, J. Sola, T. Boddaert, T. Marcelli, R. W. Adams, G. A. Morris and J. Clayden, *Angew. Chem. Int. Ed.*, 2014, **53**, 151; (e) R. W. Sinkeldam, M. H. C. J. van Houtem, K. Pieterse, J. A. J. M. Vekemans and E. W. Meijer, *Chem. Eur. J.*, 2006, **12**, 6129; (f) V. Maurizot, C. Dolain and I. Huc, *Eur. J. Org. Chem.*, 2005, 1293; (g) C. Dolain, H. Jiang, J. M. Leger, P. Guionneau and I. Huc, *J. Am. Chem. Soc.*, 2005, **127**, 12943; (h) C. Dolain, J. M. Leger, N. Delsuc, H. Gornitzka and I. Huc, *Proc. Natl. Acad. Sci. USA*, 2005, **102**, 16146; (i) N. Delsuc, T. Kawanami, J. Lefeuvre, A. Shundo, H. Ihara, M. Takafuji and I. Huc, *ChemPhysChem*, 2008, **9**, 1882; (j) A. M. Kendhal, L. Poniman, Z. Dong, K. Laxmi-Reddy, B. Kauffmann, Y. Ferrand and I. Huc, *J. Org. Chem.*, 2011, **76**, 195; (k) N. Delsuc, S. Massip, J.-M. Leger, B. Kauffmann and I. Huc, *J. Am. Chem. Soc.*, 2011, **133**, 3165; (l) S. J. Dawson, A. Meszaros, L. Petho, C. Colombo, M. Csekei, A. Kotschy and I. Huc, *Eur. J. Org. Chem.*, 2014, 4265; (m) J. L. Hou, H. Yi, X. B. Shao, C. Li, Z. Q. Wu, X. K. Jiang, L. Z. Wu, C. H. Tung and Z. T. Li, *Angew. Chem. Int. Ed.*, 2006, **45**, 796.
8. (a) J. F. Galan, J. Brown, J. L. Wildin, Z. Liu, D. Liu, G. Moyna and V. Pophristic, *J. Phys. Chem. B*, 2009, **113**, 12809; (b) J. F. Galan, C. N. Tang, S. Chakrabarty, Z. Liu, G. Moyna and V. Pophristic, *Phys. Chem. Chem. Phys.*, 2013, **15**, 11883; (c) Z. Liu, A. M. Abramyan and V. Pophristic, *New J. Chem.*, 2015, **39**, 3229; (d) Z. Liu, R. C. Remsing, D Liu, G. Moyna and V. Pophristic, *J. Phys. Chem. B*, 2009, **113**, 7041; (e) Z. Liu, A. Teslja and V. Pophristic, *J. Comput. Chem.*, 2011, **32**, 1846; (f) S. Vemparala, I. Ivanov, V. Pophristic, K. Spiegel and M. L. Klein, *J. Comput. Chem.*, 2006, **27**, 693; (g) V. Pophristic, S. Vemparala, I. Ivanov, Z. Liu, M. L. Klein and W. F. DeGrado, *J. Phys. Chem. B*, 2006, **110**, 3517.
9. A. Laio and M. Parrinello, *Proc. Natl. Acad. Sci. USA*, 2002, **99**, 12562.
10. A. Pietropaolo and T. Nakano, *J. Am. Chem. Soc.*, 2013, **135**, 5509.
11. G. Diaz Leines and B. Ensing, *Phys. Rev. Lett.*, 2012, **109**, 020601.
12. T. Qi, V. Maurizot, H. Noguchi, T. Charoenraks, B. Kauffmann, M. Takafuji, H. Ihara and I. Huc, *Chem. Commun.*, 2012, **48**, 6337.
13. (a) D. Chakrabarti and D. J. Wales, *Soft Matter*, 2011, **7**, 2325; (b) P. Tao, J. R. Parquette and C. M. Hadad, *J. Chem. Theory Comput.*, 2012, **8**, 5137.
14. H. Jiang, J. M. Leger and I. Huc, *J. Am. Chem. Soc.*, 2003, **125**, 3448.